ACS Energy LETTERS

Cite This: ACS Energy Lett. 2019, 4, 1484−1495

http://pubs.acs.org/journal/aelccp

PERSPECTIVE

Shape-Controlled Nanoparticles as Anodic Catalysts in Low-Temperature Fuel Cells

Rubén Rizo and Beatriz Roldan Cuenya*

Fritz-Haber Institute of the Max-Planck Society, D-14195 Berlin, Germany

ABSTRACT: The great dependence of the electrocatalytic activity of most electrochemical reactions on the catalytic surface area and specific surface structure is widely accepted. Building on the extensive knowledge already available on single-crystal surfaces, this Perspective discusses the recent progress made in low-temperature fuel cells through the use of the most active shape-controlled noble metal-based nanoparticles. In particular, we will focus on discussing structure−composition−reactivity correlations in methanol, ethanol, and formic acid oxidation reactions and will offer a general vision of future needs.

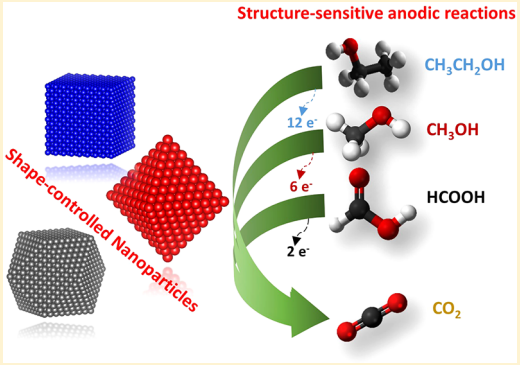

The sensitivity of electrochemical reactions to the crystallographic structure of the electrode surface is a well-established fact demonstrated during the last decades by many authors.[1] Thus, control of the exposed metal facets is essential in order to optimize their electrocatalytic activity. In this regard, the use of metal single crystals with well-defined atomic arrangements allows the systematic investigation of the correlation between surface structure, composition and reactivity.[1] Platinum (Pt) and palladium (Pd) single crystals are the most studied surfaces in electrocatalysis for energy conversion because they are the most electroactive metals toward low-temperature fuel cell oxidation reactions.[2−6] Pt and Pd possess a face-centered cubic (fcc) structure with crystallographic facets that can be depicted in a stereographic triangle (Figure 1). At the corners of the triangle there are three low-index planes, (111), (100), and (110), with coordination numbers of 9, 8, and 7, respectively, while at the edges of the triangle stepped surfaces can be found.

Because single-crystal electrodes cannot be used for realistic industrial fuel cell applications, metallic nanoparticles (NPs) uniformly dispersed on appropriate supports are being considered in order to maximize the surface/volume ratio and minimize the amount of noble metal used to reduce cost. Taking into account the knowledge extracted from fundamental single-crystal studies and the strong structure-dependent relationship observed for alcohol oxidation anodic reactions, significant effort has been dedicated to the design of shape-controlled NP electrocatalysts. Thus, in analogy with the stereographic triangle for single-crystal surfaces, small nanosized crystals can also be constructed in order to associate the crystal surface index and the NP shape (Figure 1). At the vertex of the triangle, NPs with low-index facets bonded by basal facets can be found, i.e., octahedra with {111} facets,

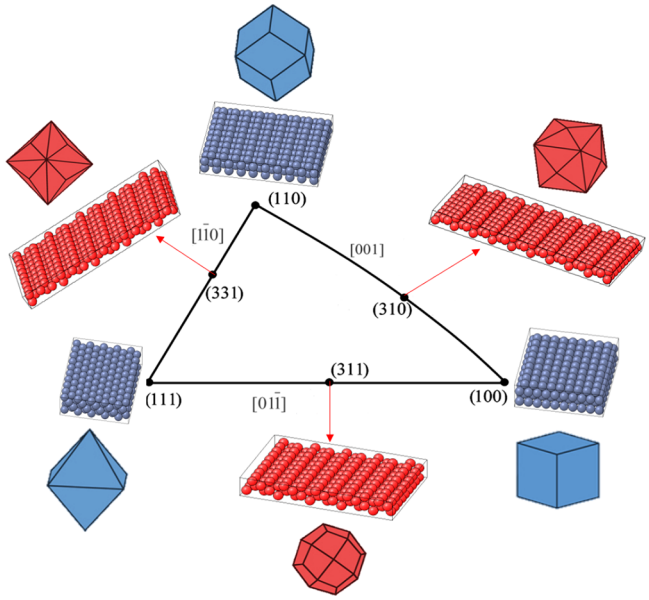

Figure 1. Stereographic triangle of fcc single-crystal surfaces with the corresponding model of the surface atomic arrangements and polyhedral nanocrystals bounded by the corresponding crystal planes. The basal planes and polyhedra bonded by low-index facets are depicted in blue, and stepped planes and polyhedra bonded by high-index facets are shown in red.

Received: March 15, 2019
Accepted: May 15, 2019
Published: May 15, 2019

DOI: 10.1021/acsenergylett.9b00565
ACS Energy Lett. 2019, 4, 1484−1495

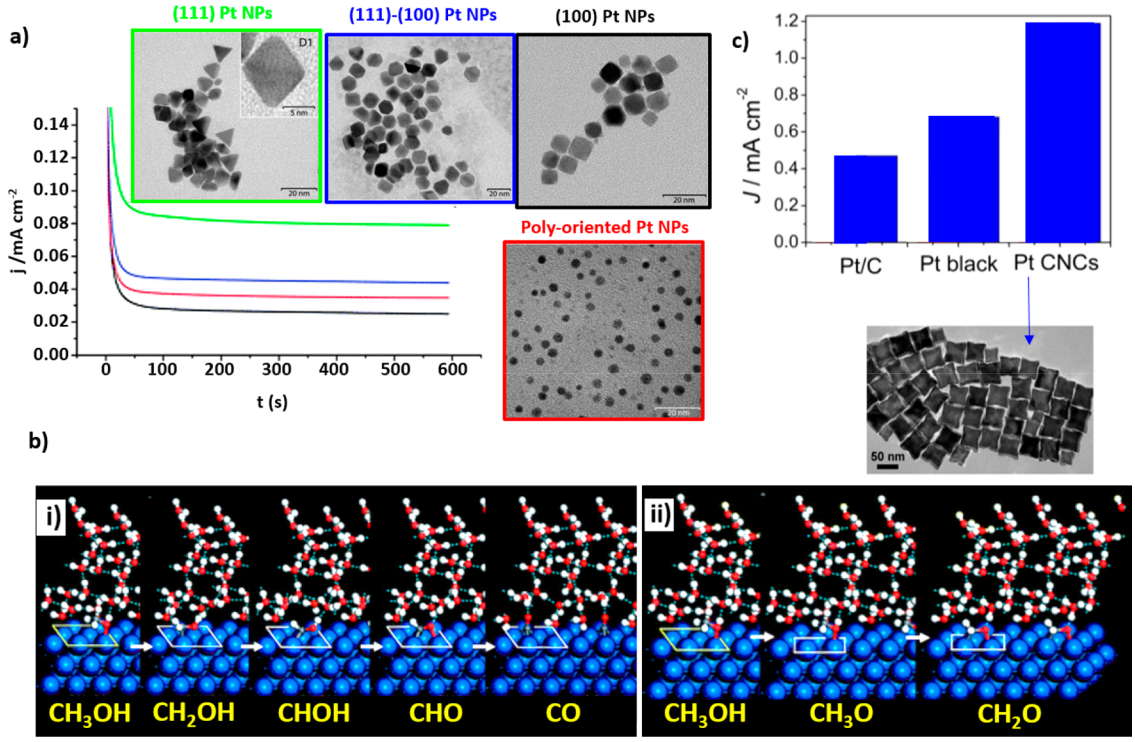

Figure 2. (a) Chronoamperometric measurements during MOR at 0.6 V for poly oriented (red line), (100) (black line), (100)−(111) (blue line), and (111) (green line) Pt NPs measured in 0.5 M H_2SO_4 + 0.5 M CH_3OH. The insets correspond to the TEM images of the samples. (b) DFT-optimized structures of the MOR intermediates on Pt(111) at 0.5 V in aqueous solution: (i) CO_{ad} via the primary path and (ii) formaldehyde via the secondary path. (c) Peak MOR current densities of Pt black, commercial Pt/C catalysts, and concave cubic Pt NPs. The inset shows a TEM image of the concave cubic Pt NPs. Reproduced with permission from ref 13, copyright 2008 Royal Society of Chemistry (a); from ref 15, copyright 2009 Royal Society of Chemistry (b); and from ref 18 (c).

nanocubes with {100} facets, and rhombic dodecahedra with {110} facets, while in the edges one can find NPs with high-index surface facets.

Among the different methods for the synthesis of shape-controlled NPs, the use of colloidal routes is the most conventional approach. These methods are characterized by the chemical reduction of the metallic precursor in the presence of a capping agent or surfactant. Unfortunately, the presence of a surfactant can also constitute a problem in electrochemical applications, because these organic molecules on the surface of the nanocatalysts might block the catalytic active sites. Therefore, good cleaning methods to remove the surfactants without perturbing the NP shape are mandatory.[7,8] Nonetheless, significant work has also been dedicated to the development of surfactant-free methods for the synthesis of shape-controlled NPs.

Additionally, the use of bimetallic or trimetallic formulations combining noble active metals with other transition metals has also been widely employed not only to reduce the cost but also to improve the performance of the catalysts. In this Perspective we will provide a brief overview of the progress described in the literature concerning the optimization of low-temperature fuel cells based on the use of multimetallic shape-controlled NPs. We will focus on the three main anodic reactions used for energy conversion, namely, the methanol electro-oxidation (MOR), ethanol electro-oxidation (EOR), and formic acid electro-oxidation reactions (FAOR).

Methanol Electro-oxidation. Pt is known to be the pure metal with the highest activity toward MOR. At Pt surfaces, methanol can be either completely oxidized to CO_2 or partially oxidized to side-products such as HCHO, HCOOH, and CO_{ad}.[9] In fact, CO_{ad} was found to be the most stable surface adsorbate leading to the deactivation of Pt surfaces. Many fundamental studies on Pt single crystals revealed that among the three Pt basal planes, the Pt(100) surface is the most active for MOR in acidic media (pH 1), whereas Pt(111) is the most active in alkaline media (pH 13).[3,10,11] Consequently, on the basis of the high activity of the Pt(100) surface in acidic electrolytes, several groups have dedicated their efforts toward the synthesis of Pt cubes with {100} low-index facets for MOR. Han et al. prepared Pt nanocubes with an average size of 3.5 nm in the presence of poly(vinylpyrrolidone) (PVP) as a surfactant and Fe ions as kinetic controllers.[12] They compared the activity of these NPs and a Pt/C commercial catalyst and found slightly higher current on the nanocubes than on the polycrystalline catalyst. However, the unexpected higher activity of the octahedral/tetrahedral NPs when compared to nanocubes was also reported (Figure 2a).[13,14] Solla-Gullon et al. attributed this fact to the presence of heterogeneities on the surface and low-coordinated surface atoms with lower poisoning rate on NPs with predominantly {111} facets as compared to nanocubes. In fact, these surface heterogeneities have been proven to play a fundamental role in the MOR mechanism. Cyclic voltammetry (CV) measurements and density functional theory (DFT) calculations on Pt(111) surfaces demonstrated that 3−4 Pt atoms on this surface are required for the primary MOR pathway involving CO_{ad} formation. On the other hand, only 1−2 atoms are needed for the direct MOR without the formation of the poisoning intermediate (Figure 2b).[15,16]

DOI: 10.1021/acsenergylett.9b00565
ACS Energy Lett. 2019, 4, 1484−1495

Thus, low-coordinated Pt atoms that might be present on non-ideal {111} surfaces could promote the direct MOR. Furthermore, motivated by the high activity observed on stepped Pt single-crystal surfaces,[17] the synthesis of Pt NPs with high-index facets was also reported.[18−20] For instance, an enhancement of the specific activity (current per unit surface area) toward MOR was obtained on concave cubic Pt NPs because of the higher surface area and higher density of step/kink sites with greater reactivity (Figure 2c).[18] However, additional systematic studies are still needed in order to compare the performance of Pt NPs with low- and high-index facets instead of using as reference polycrystalline Pt NPs.[18−20]

CV measurements and DFT calculations on Pt(111) surfaces demonstrated that 3−4 Pt atoms on this surface are required for the primary MOR pathway involving CO_{ad} formation.

Another important point to consider is the effect of the capping agents used in the synthesis of the differently shaped NPs, because some of the discrepancies observed in the literature in terms of catalytic performance might simply arise from residues on the NP surface leading to poisoning of the active sites. Significant effort has been dedicated to remove organic molecules from the surface of the catalyst without perturbing its morphology. For instance, Arán-Ais et al. carried out a chemical wash with a mix of methanol and acetone in a NaOH solution in order to remove oleylamine (OAm) and oleic acid (OA) from the surface of Pt cubes[7] (Figure 3a). However, the removal of the surfactants is difficult and often entails a change in the surface morphology of the catalyst. Consequently, some groups have developed surfactant-free methods for the synthesis of shaped NPs for MOR and reported higher activity for the Pt NPs free of capping agents when compared to those synthesized using conventional methods involving polymers (Figure 3b).[21,22]

Besides Pt, Pd has also been studied for MOR and found to present a strong Pd surface-dependence. However, shape-controlled Pd NPs were less extensively investigated, and work on Pd cubes, concave Pd cubes, and star-like concave Pd NPs can be mainly found.[23−25] All of them showed activity higher than that of the samples containing NPs with mixed facets; however, insufficient information is available to conclude what is the optimum Pd shape for MOR. As was mentioned before for the Pt NPs, the complete removal of the capping agents from the Pd NPs has also been a topic of great interest. Some groups tried electrochemical cycling the samples to high potentials, but they found modifications in the surface structure. Ascorbic acid has also been used as a reducing agent in the absence of an organic capping agent.[24] Nevertheless, NPs with larger sizes (>50 nm) were generally obtained, which results in a low "Pd utilization" (low ratio of surface atoms to bulk). Thus, further efforts must be made in order to get cleaner and smaller shape-controlled Pd NPs as well as the systematic comparison of a larger variety of shapes to be able to optimize the Pd catalysts by exposing the most active Pd facets for MOR.

The improvement in activity of pure Pt catalysts due to the presence of a second transition metal is thought to be a combination of a bifunctional mechanism and ligand effects. Following the bifunctional effect, a partially oxidized transition metal can provide oxygenated species which allow the complete oxidation of methanol to CO_2. According to ligand effect considerations, the second metal leads to changes in the Pt electronic structure which entail the weakening of the Pt-CO_{ads} bond.[26] It is widely accepted that Pt−Ru catalysts are the most active bimetallic catalysts for MOR.[27−29] However, other less expensive metals, especially 3d transition metals, such as Cu, Co, or Sn, have also been employed for the synthesis of bimetallic (Pt−M) shape-controlled NPs for MOR.[30−34] All of these studies agreed with respect to the fact

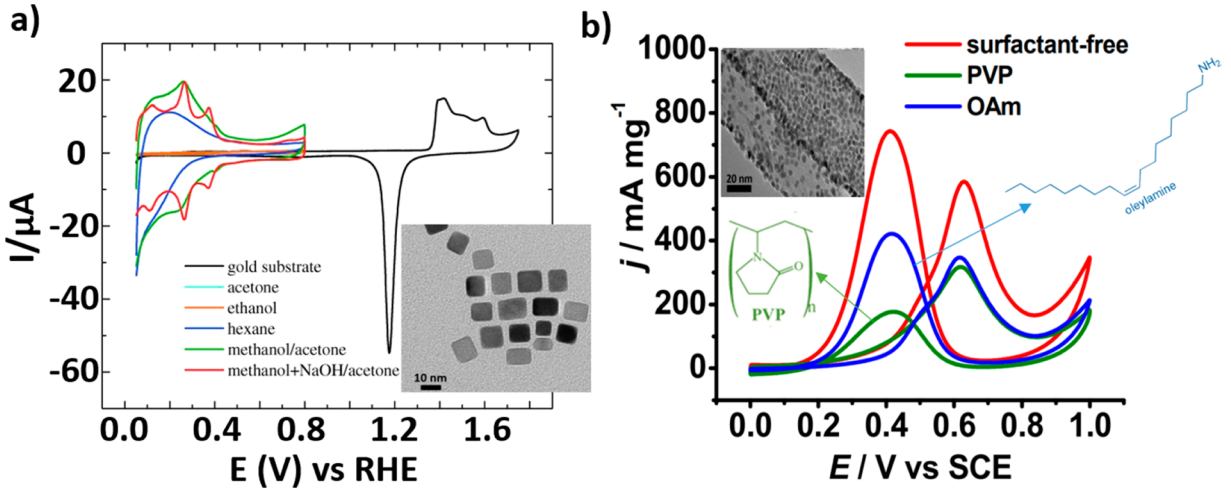

Figure 3. (a) Voltammetric profiles of (100)-Pt NPs supported on gold. The NPs were cleaned with acetone (cyan line), ethanol (orange line), hexane (blue line), methanol/acetone (green line), and methanol enriched with sodium hydroxide/acetone (red line). Data were acquired in a 0.5 M H_2SO_4 solution with a sweep rate of 50 mV s^{-1}. The inset corresponds to a TEM image of the Pt nanocubes synthesized using OAm and OA as capping agents. (b) Cyclic voltammograms during MOR from Pt nanocubes synthesized with and without surfactants and supported on carbon nanotubes (CNT). Data were acquired in an aqueous solution of 0.5 M H_2SO_4 with 1 M methanol. The inset corresponds to a TEM image of the cubes synthesized without surfactant. Reproduced with permission from ref 7, copyright 2015 Wiley (a); and ref 21, copyright 2012 Royal Society of Chemistry (b).

DOI: 10.1021/acsenergylett.9b00565
ACS Energy Lett. 2019, 4, 1484−1495

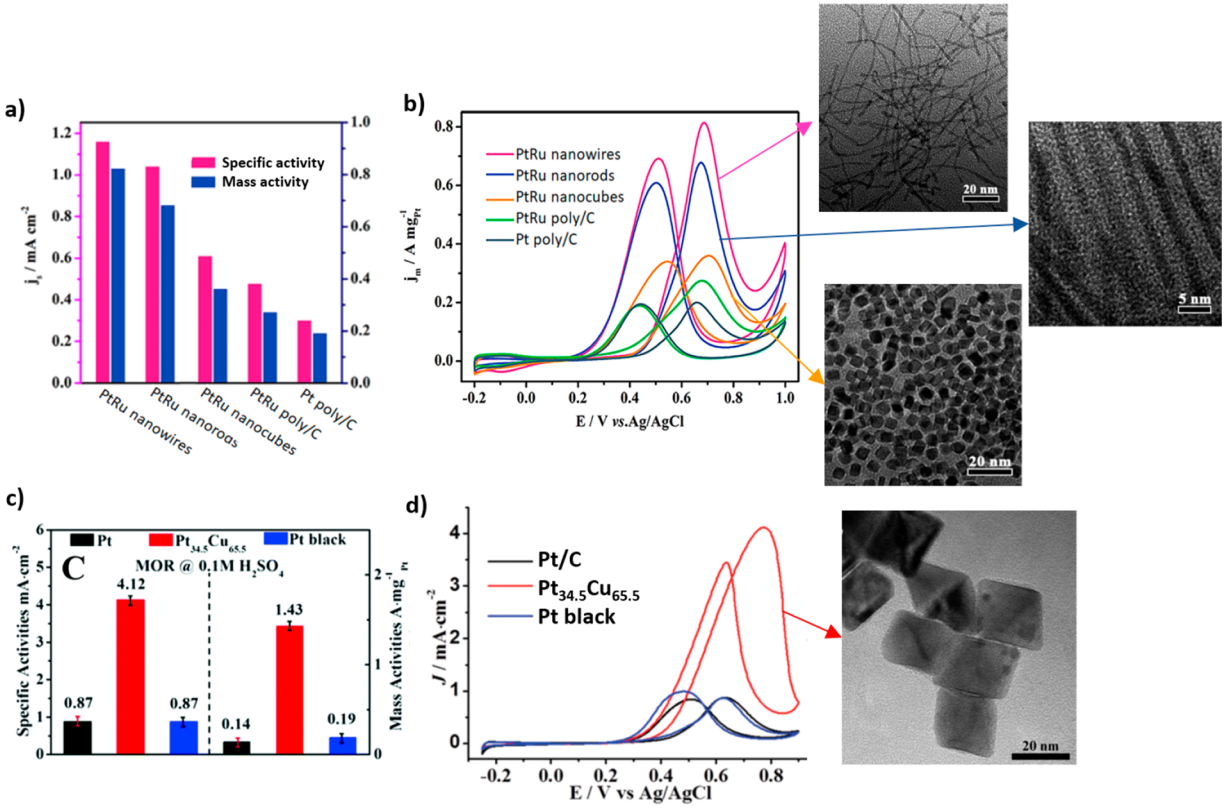

Figure 4. (a) Histograms of the mass and specific activities of shape-controlled Pt−Ru and commercial Pt/C catalysts and (b) CV curves of the different catalysts for MOR in a 0.1 M $HClO_4$ + 0.5 M CH_3OH solution at a sweep rate of 50 mV s^{-1}. (c) MOR specific and mass activity for the as-synthesized Pt cubes, $Pt_{34.5}Cu_{65.5}$ octahedra, and commercial Pt black. (d) MOR cyclic voltammograms of commercial Pt/C, Pt black, and PtCu octahedral NPs in 0.1 M H_2SO_4 + 0.5 M CH_3OH (scan rate 50 mV s^{-s}). The insets correspond to the TEM images for the NPs synthesized in refs 27 and 32. Reprinted from ref 27 (a and b) and reproduced with permission from ref 32, copyright 2018 Royal Society of Chemistry (c and d).

that the transition metal enhances the activity of the Pt catalysts. Furthermore, in analogy with the conclusions extracted for pure Pt NPs, a superior methanol oxidation activity and CO-poisoning tolerance were found for NPs with a higher concentration of {111} facets, regardless of the nature of the second metal. For example, Huang et al. recently reported the synthesis of ultrathin PtRu nanocrystals with tunable morphology (nanowires, nanorods, nanocubes, and NPs) by using hexadecyldimethylbenzyl ammonium chloride (HDBAC), cetyltrimethylammonium bromide (CTAB), dimethyldioctadecylammonium chloride (DDAC), and OAm as surfactants.[27] They demonstrated that {111}-terminated PtRu nanowires exhibit much higher stability and electroactivity than Pt−Ru nanocubes and commercial Pt/C, respectively (Figure 4a,b). In general, nanowires stand out for their high surface area, which results in high mass activity. However, the authors demonstrated that this catalyst shows not only superior mass activity but also higher specific activity than other shaped catalysts with the same composition. Wang's group also demonstrated the high electroactivity of these particular facets by using octahedral $Pt_{34.5}Cu_{65.5}$ NPs with CTAB as a capping agent (Figure 4c,d). They found a 4.7 times higher specific activity and 7.5 times higher mass activity than that of commercial Pt black.[32]

Although the reason why the Pt {111} facets confer higher activity to the bimetallic catalysts is yet unclear, some authors reported a weaker interaction between the Pt atoms on this surface and unreactive oxygenated species on the {111} facets of the bimetallic catalysts. The increase in the number of active sites for the adsorption of oxygen would favor the oxidation of CO adsorbed on Pt, resulting in better electrocatalytic activity than bimetallic NPs with predominantly {100} facets and those with irregular facets. Moreover, Pt-based NPs containing high-index facets have also been extensively studied, even in a greater extent than pure Pt NPs with the same shape. Cu, Ni, Pd, or Ru have been employed for the synthesis of diverse shaped NPs such as concave cubes, tetrahexahedral, trapezohedral, or rhombic dodecahedral NPs.[29,31,35,36] All of the NPs with these special facets showed much higher activity than Pt-based NPs with mixed facets, regardless of the nature of the second metal. However, further comparison with low-index facet NPs is still missing.

Ethanol Electro-oxidation. The EOR has been less extensively studied than the other two reactions because of its higher complexity. However, interest in this reaction has increased during the last decades because ethanol can be obtained from renewable sources (bioethanol) and is less toxic, its corrosive power is low, and its complete oxidation to CO_2 releases 12 electrons (2 electrons for FAOR and 6 electrons for MOR). However, for the complete oxidation of ethanol it is necessary to break the C−C bond, which is a complicated process which needs high overpotentials.[37] Many groups have demonstrated the great influence of the Pt surface structure in the EOR mechanism. Similar to the case of MOR, Pt single-crystal studies showed that the Pt(100) surface is the most active for EOR in acidic media, whereas Pt(111) is the one which shows

DOI: 10.1021/acsenergylett.9b00565
ACS Energy Lett. 2019, 4, 1484−1495

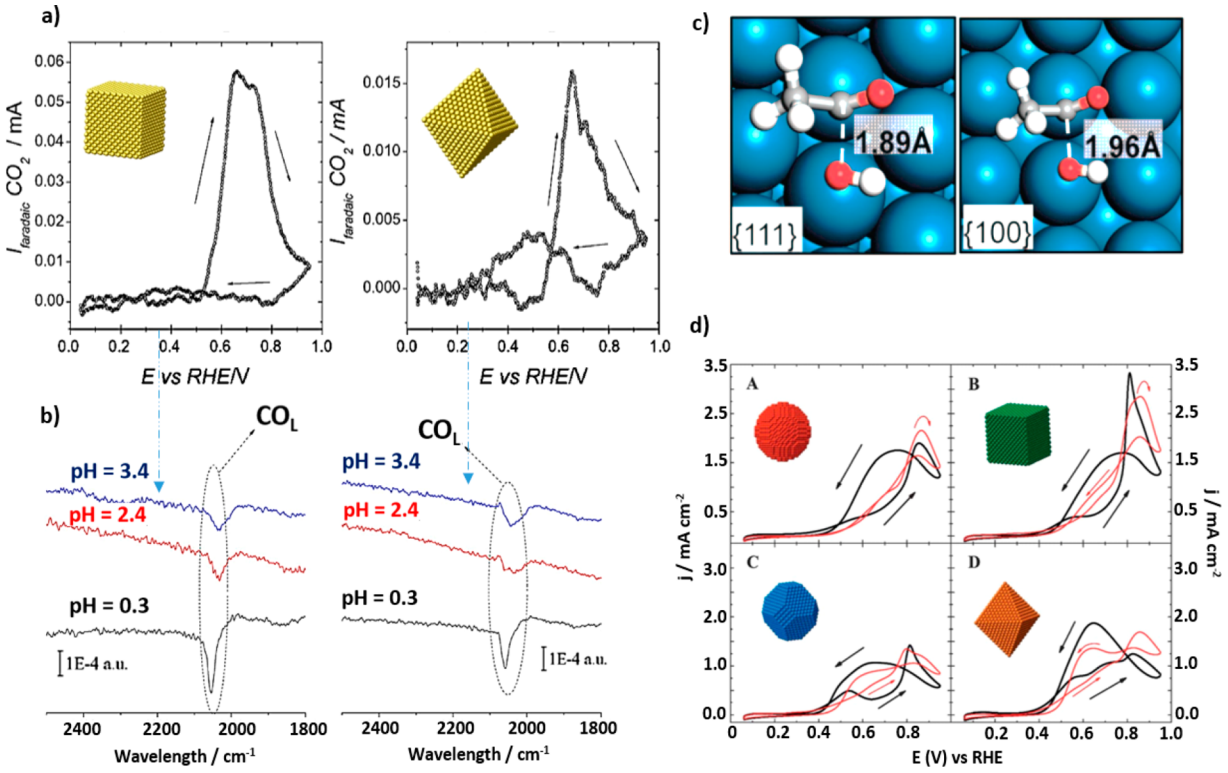

Figure 5. (a) CO_2 formation currents extracted from DEMS experiments and (b) ATR spectra obtained at E = 0.4 V vs RHE for Pt(100) and Pt(111) NPs in 0.05 M CH_3CH_2OH + 0.5 M H_2SO_4. (c) Transition-state structures of the reaction $CH_3CO + OH \rightarrow CH_3COOH$ on Pt(111) and Pt(100) surfaces. (d) Ethanol oxidation (first cycle) on (A) (poly)Pt, (B) (100) Pt, (C) (100)−(111) Pt, and (D) (111) Pt NPs in 0.5 M H_2SO_4 + 0.2 M CH_3CH_2OH (black line) and 0.1 M $HClO_4$ + 0.2 M CH_3CH_2OH (red line). Sweep rate: 50 mV s^{-1}. Reproduced with permission from ref 41, copyright 2016 Elsevier (a and b); reprinted from ref 42 (c); and reproduced with permission from ref 43, copyright 2013 Royal Chemical Society (d).

the highest activity in alkaline media among the three Pt basal planes.[38,39] In order to gain in-depth knowledge about the role of the shape in EOR over Pt NPs, Feliu et al. employed spectroelectrochemical techniques such as differential electrochemistry mass spectrometry (DEMS) and in situ Fourier transform infrared spectroscopy (FTIR).[40,41] Spherical (4 nm), cubic, and octahedral (8−10 nm) Pt NPs were synthesized by a water-in-oil microemulsion in the case of the spherical NPs and a colloidal method with NaPA as capping agent in the case of the cubic and octahedral NPs. The incomplete oxidation of ethanol was found to be dominant, but the ratio between the complete and incomplete oxidation was demonstrated to be surface-dependent. For example, whereas octahedral NPs with predominantly {111} facets showed almost exclusively acetic acid formation and a very low amount of CO_2, cubic NPs with {100} facets were found to be more active for breaking the C−C bond to form CO_2 as a final product (Figure 5a,b). The latter was confirmed theoretically by Wang et al. through the determination of the transition states formed during the reaction. They found that, on Pt(100) surfaces, the oxidation reaction of the acetyl group (CH_3CO) to form acetic acid is significantly inhibited when compared to the Pt(111) surface (the transition states are shown in Figure 5c), while the dehydrogenation of this group and the breaking of the C−C bond becomes more feasible.[42] Furthermore, in terms of electroactivity, cyclic voltammetry experiments showed higher maximum current for Pt nanocubes than for Pt octahedra (Figure 5d).[43]

Whereas octahedral NPs with predominantly {111} facets showed almost exclusively acetic acid formation and a very low amount of CO_2, cubic NPs with {100} facets were found to be more active for breaking the C−C bond to form CO_2 as a final product.

Moreover, similar to the case of MOR and motivated by the good performance of stepped Pt single-crystals surfaces, a number of groups have synthesized Pt NPs with high-index facets.[44−48] For example, Sun and co-workers[44] electrochemically synthesized tetrahexahedral (THH) Pt NPs with {730}, {210}, and {520} high-index facets and compared their activity to that of Pt nanospheres and commercial Pt/ETEK catalysts. Current-transient curves acquired at 0.3 V vs SCE showed that the stationary currents of the THH Pt NPs (normalized by the Pt surface area) are enhanced, being 230% higher than those of the nanospheres and 330% of that of the Pt/ETEK catalysts. However, most of these works describe NPs with quite large size (>50 nm), which results in a low Pt utilization. Smaller Pt NPs with high-index facets were obtained by applying a short square-wave potential to 10 nm Pt nanocubes that were found to transform into THH nanocrystals with sizes from 6 to 20 nm.[45] A remarkable increase in activity toward EOR was observed after this treatment as compared to the as-prepared Pt nanocubes and commercial Pt NPs. High activity for EOR

DOI: 10.1021/acsenergylett.9b00565
ACS Energy Lett. 2019, 4, 1484−1495

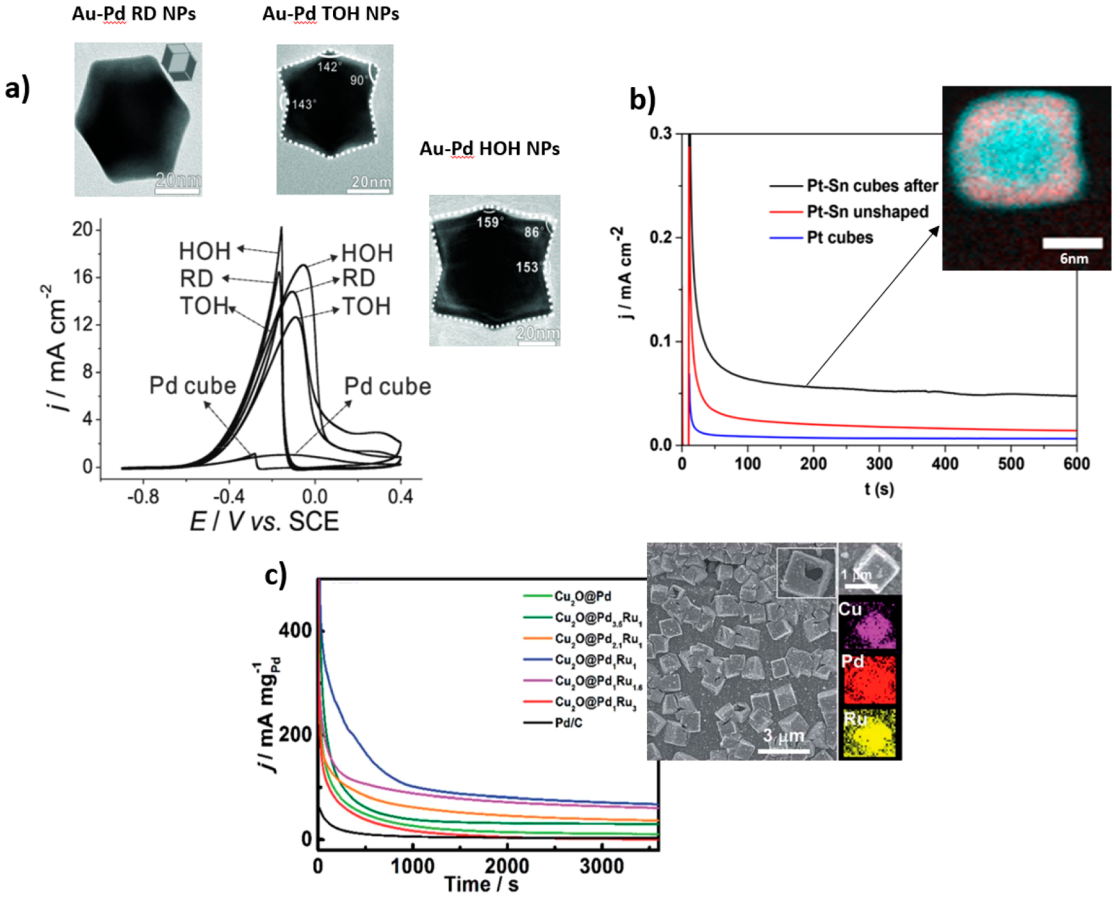

Figure 6. (a) CV curves measured on Au−Pd alloy NPs with RD, HOH, and TOH morphologies and Pd-cubes measured in 0.1 M NaOH + 0.1 M EtOH (scan rate: 50 mV s^{-1}). The insets correspond to the TEM images of the Au−Pd nanocrystals. (b) Current transients at 0.50 V of Pt−Sn nanocubes (black), unshaped Pt−Sn nanoparticles (red), and Pt-cubic NPs (blue) in Ar-purged 0.5 M H_2SO_4 + 1 M EtOH solution. The inset corresponds to the STEM-EELS data of the Pt−Sn cubic NPs with Sn in red and Pt in cyan. (c) Chronoamperometry curves of Cu_2O@Pd_xRu_y and Pd/C measured in a 1.0 M EtOH + 1.0 M KOH solution. The inset corresponds to the SEM image of Cu_2O@Pd_1Ru_1 NPs and the elemental mapping of an individual NP. Reproduced with permission from ref 48, copyright 2013 Wiley (a); reprinted from ref 53 (b); and reproduced with permission from ref 58, copyright 2016 Royal Chemical Society (c).

has also been reported for Rh and Pd NPs with high-index facets exposed.[49,50] However, the activity of both metals is much worse when compared to Pt in acidic media,[51,52] although some studies have demonstrated that Pd exhibits even a higher activity than Pt for EOR in alkaline media.[51]

In spite of the high activity shown by pure noble metal NPs with exposed high-index facets, fewer works describe the EOR over analogous bimetallic NPs.[46−48] For instance, Zhang et al. studied Au−Pd nanocrystals with rhombic dodecahedral (RD), trisoctahedral (TOH), and hexoctahedral (HOH) shape by controlling the amount of surfactant in the synthesis[48] and found that given analogous NP size and composition, different EOR activities could be achieved: HOH > RD > TOH (Figure 6a). This difference in activity was attributed to the different surface energy of the NPs; the catalysts with higher surface energy are the ones which possessed the highest catalytic activity.

On the other hand, Pt-based cubic NPs with predominantly {100} facets, such as Pt−Sn, Pt−Rh, and Pt−Pd, have been more widely studied.[53−56] The low price of Sn in comparison with noble metals as well as the higher capacity of Sn to lower the onset potential for EOR and increase the CO-tolerance of Pt make Pt−Sn formulations promising catalysts toward EOR. Pt−Sn nanocube catalysts from Abruña's group[53] composed of a Pt-rich core, a Sn-rich subsurface layer, and a Pt-skin surface structure were found to be highly active and stable during EOR (Figure 6b).

Despite the high difficulty associated with the synthesis of NPs with a particular shape containing three different metals, good performance in terms of electroactivity toward EOR has been described for trimetallic shape-controlled NPs. For instance, Strasser's and Cheng's groups obtained octahedral Pt−Ni−Rh and hollow-cubic Cu_2O@Pd_xRu_x NPs, respectively.[57,58] In particular, Cheng's group found an enhanced activities on their hollow-cubic Cu_2O@Pd_xRu_x NPs trimetallic catalysts when compared to polycrystalline Pd NPs, and the catalysts with Pd:Ru atomic ratio of 1:1 showed the highest electroactivity (Figure 6c).[58]

Formic Acid Electro-oxidation. FAOR is a model two-electron-transfer reaction that is promising for low-temperature fuel cell applications. The existence of a dual mechanism for the FAOR is widely accepted: (i) direct oxidation to CO_2 by the formation of an adsorbed active intermediate of yet unclear nature, or (ii) an indirect pathway via CO_{ads} formation (poisoning intermediate) and the subsequent oxidation to CO_2 at high overpotentials. On Pt surfaces, many studies have demonstrated that both pathways take place, although the mechanism is surface-structure-dependent.[13] However, on Pd

DOI: 10.1021/acsenergylett.9b00565
ACS Energy Lett. 2019, 4, 1484−1495

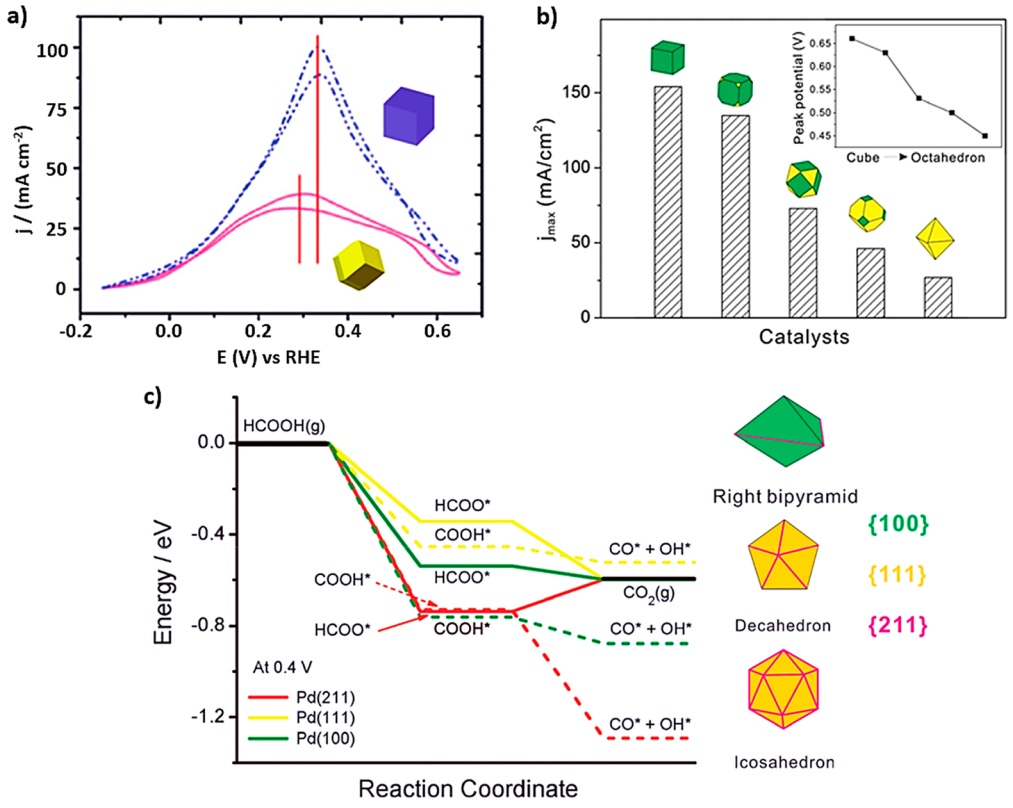

Figure 7. (a) CV curves of Pd rhombic dodecahedral and cubic NCs in 0.5 M H_2SO_4 + 0.5 M HCOOH (scan rate, 50 mV s^{-1}). (b) Maximum current densities of formic acid oxidation over Pd polyhedrons enclosed by {111} and {100} facets in different proportions in 0.1 M $HClO_4$ and 2 M HCOOH at a scan rate of 10 mV s^{-1}. (c) DFT-calculated thermochemical potential energy surfaces for formic acid oxidation at 0.4 V through HCOO-mediated (solid lines) and COOH-mediated (dashed lines) pathways on Pd(211) (red), Pd(111) (yellow), and Pd(100) (green). The right insets depict the models to describe the different shape-controlled Pd nanocrystals and the facets exposed on their faces and twin boundaries. Reproduced with permission from ref 61, copyright 2012 Royal Chemical Society (a); from ref 62, copyright 2012 Royal Chemical Society (b); and from ref 68, copyright 2015 Wiley (c).

surfaces, the dehydration step of formic acid and the subsequent CO_{ads} formation do not take place, and the reaction occurs only through the direct pathway.[59] Furthermore, the onset potential for the FAOR on Pd is lower than on Pt surfaces, and this is the reason why FAOR has been more extensively studied on Pd, in contrast to EOR and MOR. Consequently, the preparation of shape-controlled Pd NPs has been extensively investigated. Many groups have synthesized Pd NPs enclosed by {100} and {111} facets and demonstrated that the activity for FAOR systematically improved for NPs having a higher fraction of {100} facets.[60−62] The latter is in agreement with fundamental single-crystal studies which established that Pd(100) is the most active surface among the three basal planes. However, Shao et al. contradicted this statement and reported similar FAOR activities for cubes and octahedral Pd NPs synthesized using PVP as capping agent.[63] However, this result might be explained by residues from the synthesis contaminating the NP surface as suggested by the blank profiles for both Pd NPs reported, which clearly differ from those of clean Pd surfaces. This finding yet again emphasizes the importance of the use of a good cleaning protocol for removing organic surfactants from the NP surface.

Furthermore, in contrast to the performance of Pt toward MOR and EOR, the presence of high-index facets does not seem to improve the behavior of the Pd NPs in terms of activity, when compared with Pt cubes (Figure 7a,b).[61,62]

On the basis of in situ FTIR, DFT calculations, and/or cyclic voltammetry, it was proven that the main contribution to the electro-oxidation of formic acid on Pd(100) is the bridge formate on Pd terraces.[64] This surface is able to stabilize at least two bridge formate species, which entails a higher electro-oxidation activity toward FAOR than facets with other geometries. However, more recently other studies revealed that twin planes or twin defects in Pd catalysts can promote the HCOO formation pathway. This pathway is energetically less favorable for the formation of poisoning CO_{ads} on the surface, which results in higher electrocatalytic activity toward FAOR, even higher than that of NPs with predominantly {100} facets with no twin defects.[65−67] In this sense, Choi et al. modeled twin defects on the surface of a right pyramid, a decahedron, or an icosahedron as Pd(211) surfaces and the terrace in the defect zone as a Pd(111) or Pd(100) surface by DFT. It was observed that the formation of CO is reduced on Pd(211) if compared to both Pd(100) and Pd(111), retaining a higher fraction of the defect sites free of CO for FAO (Figure 7c).[68]

Despite the lower activity and higher price of Pt as compared to Pd, a high number of shape-controlled Pt NPs have also been reported for the FAOR.[13,18,69] Among Pt NPs with low-index facets, Pt nanocubes with {100} facets showed the highest normalized currents in the negative-going scan but very low stationary currents during the chronoamperometry due to the fast deactivation by CO poisoning. However, much better performance in terms of activity and CO-tolerance was

DOI: 10.1021/acsenergylett.9b00565
ACS Energy Lett. 2019, 4, 1484−1495

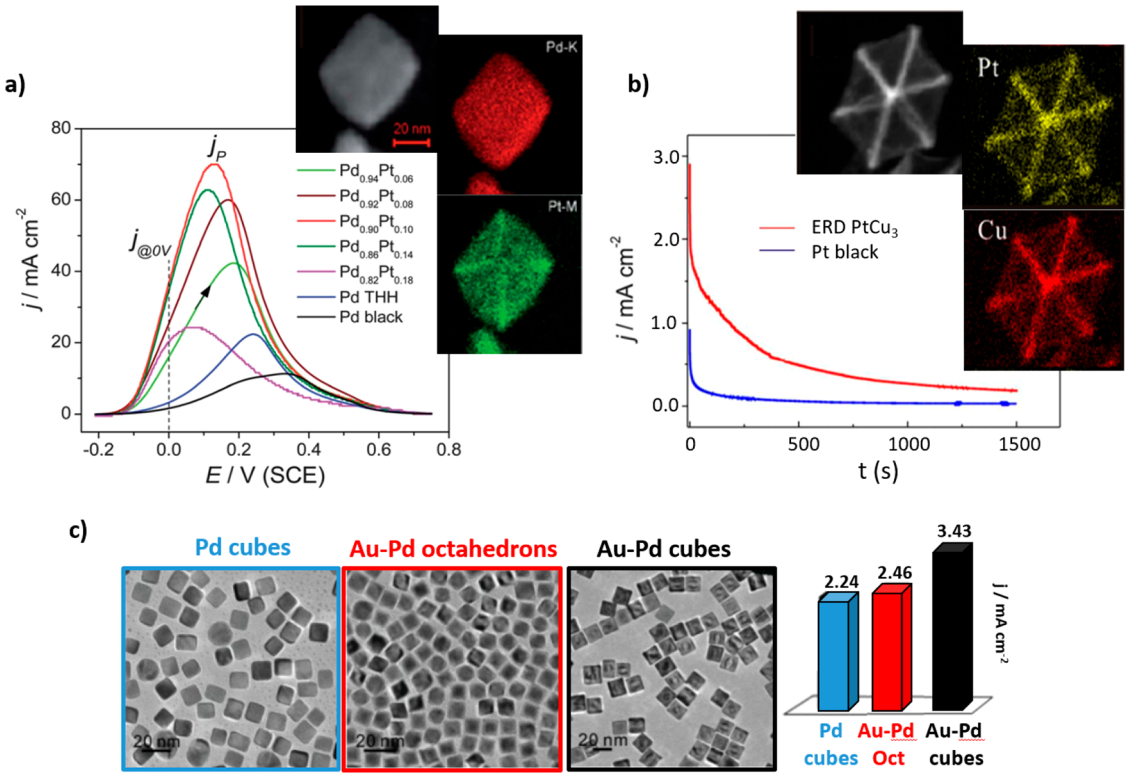

Figure 8. (a) Comparison of current−potential curves of THH Pd−Pt NCs, Pd THH, and commercial Pd black toward formic acid electro-oxidation in 0.25 M HCOOH + 0.25 M $HClO_4$ (scan rate, 50 mV s^{-1}). The inset corresponds to a STEM image and EDS elemental mapping of Pd and Pt in a THH $Pd_{0.90}Pt_{0.10}$ NP. (b) Chromoamperometric results of HCOOH oxidation on excavated rhombic dodecahedral (ERD) $PtCu_3$ and commercial Pt black in 0.5 M H_2SO_4 + 0.25 M HCOOH solution. The inset shows a STEM image and EDS elemental maps of Cu and Pt in a $PtCu_3$ ERD NP. (c) TEM images and column charts of current peak densities for formic acid electro-oxidation in a 0.5 M H_2SO_4 and 0.5 M HCOOH solution (scan rate, 100 mV s^{-1}). Reproduced with permission from ref 76, copyright 2012 Royal Chemical Society (a); reprinted from ref 74 (b); and reproduced with permission from ref 80, copyright 2013 Wiley (c).

found with Pt NPs with high-index facets, as was also the case for EOR and MOR.

Despite the fact that Pd is the most active metal for FAOR, only a few works have been reported on shape-controlled bimetallic Pd NPs, whereas bimetallic shaped Pt NPs have been more extensively studied. For instance, the selective decoration of low-index shape-controlled Pt NPs by adatoms of a different metal (Bi, Pd, Sb, and Tl) has been used to study the influence of the secondary metal on the activity and/or selectivity of bare substrates toward the FAOR.[70−73] An improvement in the electrocatalytic activity was obtained when Pt {100} nanocube surfaces were modified by Pd and Tl as well as when Bi and Sb were added to Pt octahedral NPs with predominantly {111} facets. It is worth noting that not only the peak potential but also the peak intensity values are different in all of these systems. Thus, whereas the modification of Pt nanocubes with Pd shifts the onset potential for FAOR to much lower potential values but without improving the maximum current, the decoration of Pt octahedral NPs enhances the electrocatalytic activity of pure Pt catalysts in terms of higher maximum currents. Superior activity toward FAOR was also described for high-index facet Pt NP catalysts modified by Au, Bi, Pd (Figure 8a), or Cu (Figure 8b). All of these studies showed better activity than Pt-based NPs with low-index facets.[74−78]

Regarding shaped bimetallic Pd-based NPs, a combination of Pd with Rh forming a core−shell type structure was investigated, but lower activities were obtained as compared to pure Pd cubes.[79] Pd−Au nanocubes showed higher activities than Pd cubes and Pd and Pd−Au octahedral NPs (Figure 8c).[80] Furthermore, Pd−Cu tripods synthesized by Xia's group displayed much higher activity as compared to Pd polycrystalline NPs.[81] They attributed the good performance to highly active {211} facets exposed on the catalyst as well as to an optimal density of Cu atoms on the surface for good oxidation of adsorbed intermediates. In our opinion, despite the high activity and low cost of Cu, which makes this work promising, the low stability of Cu in acidic media, as well as the poor comparison of this catalyst with other shape-controlled Pd−Cu NPs, is something which still needs further clarification.

Outlook and Future Research Opportunities. It is widely accepted that anodic reactions for low-temperature fuel cells are strongly dependent on the catalyst surface structure. Thus, it is essential to control the exposed facets of the catalysts. To fulfill this purpose, shape-controlled NPs can be synthesized by different methods. However, several important aspects must be considered in order to obtain optimum catalysts with the highest activity and selectivity to price ratio. In the first place, it would be favorable if the nanoparticle synthesis method leading to shape-controlled nanoparticles were of an electrochemical nature, because this would facilitate their large-scale production without the presence of detrimental strongly bound surface ligands, as well as a prompt utilization as electrocatalyst by a simple exchange of the electrolyte.[44,49,50,82] Second, the electrochemical synthesis as well as testing should be combined with in situ and operando chemical and physical

DOI: 10.1021/acsenergylett.9b00565
ACS Energy Lett. 2019, 4, 1484−1495

characterization techniques. The latter will allow a better control of the formation of certain facets in the NPs, will help improve the uniformity of the NP shapes, and will ultimately contribute to enhancing the current understanding of the morphological and chemical evolution of the NPs taking place under different electrochemical reaction conditions. Such knowledge is key in order to be able to tune structure-sensitive reactions such as those involved in low-temperature fuel cells. For this purpose, the further development and utilization of microscopy and spectroscopy methods for monitoring electrified liquid interfaces in situ and under operando conditions are key. Among the most promising methods one could feature EC-AFM, L-TEM, Raman and infrared spectroscopy as well as X-ray diffraction and X-ray absorption spectroscopy, for this aim. In the applied aspect, some points must be considered: (1) The facet-dependent activity must be better studied to gain insight into which is the most active metal facets that should be exposed. (2) The bimetallic and/or trimetallic formulation should be tuned in order to achieve the highest possible activity with the lowest content of noble metal (lowest price). (3) The utilization of the noble metal must be optimized, i.e., the ratio of surface to bulk atoms must be enhanced. For this purpose, the synthesis of NPs with concave facets and/or small sizes is recommended. (4) A proper method to remove the organic polymers often employed as capping agents after synthesis without perturbing the surface of the NPs and/or the use of surfactant-free synthesis approaches should be considered. (5) The development of techniques for mass production, ideally based on theoretical predictions as well as state-of-the-art technical innovations, is also needed.

In general, higher activity was found on Pt NPs with high-index facets than on low-index facets for MOR and EOR reactions in alkaline or acid electrolytes. In particular, Pt−Ru and Pt−Sn NPs have been found to be the most active bimetallic combinations for MOR and EOR, respectively. Nevertheless, it is surprising that to date not much effort has been dedicated to the synthesis of high-index facet NPs with these formulations, although many works have demonstrated that, in comparison with their low-index counterparts, the high-indexed NPs exhibit special surface structures that generally lead to superior catalytic performance toward the former two reactions. Most of the works related to these special structures have focused on the synthesis of NPs containing predominantly $\{hk0\}$ $(h > k > 0)$ facets, like THH NPs with {310}. However, many other stepped surfaces are yet to be explored. In addition, most of the syntheses described for the preparation of such shapes are based on electrochemical methods, which allowed the formation of NPs with relatively large sizes (i.e., lower surface area). Thus, the exploration of the square-wave potential parameters that would result in smaller nanocrystal sizes with high-index facets and sizes comparable to those of commercial catalysts would be essential. The latter should be combined with the development of alternative chemical preparations with the ultimate goal of having a robust but facile synthesis leading to morphologically and chemically stable electrocatalysts.

On the other hand, Pd has been found to be more active than Pt toward FAOR. Unlike the observations made for MOR and EOR, high-index facets showed lower activity for FAOR than low-index facets, with monometallic Pd nanocubes exhibiting the highest activity. However, an improvement in the activity of Pd NPs with predominantly {100} facets was shown when twin defects were available in the single-crystalline surface. Furthermore, besides the extensive study of shape-controlled Pd NPs, multimetallic Pd-based NPs have not yet been broadly investigated for this reaction, and the limited data available so far are not very promising. Thus, further research efforts must be oriented toward a better understanding of Pd-based nanocubes for FAOR.

Furthermore, although a number of methods have been described for the removal of the capping agents from the surface of the NPs, in addition to surfactant-free synthetic approaches, these aspects should be additionally improved. In fact, most of the cleaning protocols entail disordering the surface or they do not result in the complete removal of the organics. Unfortunately, most of the alternative methods to the use of polymers proposed to date are limited, allowing the synthesis of large-size NPs and/or NPs with not so well-defined shape.

Summarizing, although the development of alternatives to fossil fuels for automotive applications has been gaining significant attention during the last years, more inexpensive catalysts with proven enhanced stability are still needed in order to foster the commercialization of such technology. In terms of durability improvements, traditional Pt and Pd catalysts tend to deactivate after short working-time periods, and the cost of these noble metals is high. Thus, unquestionably, the main challenge for the near future will be the improvement of the low-temperature fuel cells lifetime and the achievement of a reduction in the cost of the catalyst. In this sense, the synthesis of highly active and cheaper shape-controlled NPs with the lowest possible content of the noble metal is expected to have a great impact on the development of such devices in the upcoming years. Nevertheless, further efforts must focus on the development of alternative materials and synthetic routes in order to be able to tune the electrocatalytic performance for alcohol oxidation reactions at the atomic level.

AUTHOR INFORMATION

Corresponding Author

*E-mail: roldan@fhi-berlin.mpg.de.

ORCID

Rubén Rizo: 0000-0001-8161-2989

Beatriz Roldan Cuenya: 0000-0002-8025-307X

Notes

The authors declare no competing financial interest.

Biographies

Rubén Rizo: obtained his B.Sc. in Chemistry from the University of Alicante (Spain) in 2011 and his Ph.D. at the University of la Laguna in 2017. He is now a postdoctoral researcher in the Department of Interface Science at the Fritz-Haber Institute of the Max Planck Society (Berlin, Germany).

Beatriz Roldan Cuenya completed her B.S. in Physics from the University of Oviedo, Spain in 1998. She obtained her Ph.D. from the Department of Physics of the University of Duisburg-Essen (Germany) in 2001. She became a postdoctoral scholar in the Department of Chemical Engineering at the University of California Santa Barbara (2001−2003). In 2004, she joined the Department of Physics at the University of Central Florida (UCF) as Assistant Professor where she moved through the ranks to become a full professor in 2012. In 2013, she became a chair professor of Solid State Physics in the Department of Physics, Ruhr-University Bochum

DOI: 10.1021/acsenergylett.9b00565
ACS Energy Lett. 2019, 4, 1484−1495

(2013−2017). Currently, she is the director of the Department of Interface Science at the Fritz-Haber Institute of the Max Planck Society (Berlin, Germany).

■ ACKNOWLEDGMENTS

This work was funded by the European Research Council under grant ERC-OPERANDOCAT (ERC-725915).

■ REFERENCES

(1) Climent, V.; Feliu, J. M. Thirty Years of Platinum Single Crystal Electrochemistry. *J. Solid State Electrochem.* **2011**, *15* (7−8), 1297.
(2) Lai, S. C. S.; Koper, M. T. M. Ethanol Electro-Oxidation on Platinum in Alkaline Media. *Phys. Chem. Chem. Phys.* **2009**, *11* (44), 10446−10456.
(3) Xia, X. H.; Iwasita, T.; Ge, F.; Vielstich, W. Structural Effects and Reactivity in Methanol Oxidation on Polycrystalline and Single Crystal Platinum. *Electrochim. Acta* **1996**, *41* (5), 711−718.
(4) Lamy, C.; Leger, J. M.; Clavilier, J.; Parsons, R. Structural Effects in Electrocatalysis: A Comparative Study of the Oxidation of CO, HCOOH and CH3OH on Single Crystal Pt Electrodes. *J. Electroanal. Chem. Interfacial Electrochem.* **1983**, *150* (1−2), 71−77.
(5) Paredis, K.; Ono, L. K.; Mostafa, S.; Li, L.; Zhang, Z.; Yang, J. C.; Barrio, L.; Frenkel, A. I.; Cuenya, B. R. Structure, Chemical Composition, and Reactivity Correlations during the in Situ Oxidation of 2-Propanol. *J. Am. Chem. Soc.* **2011**, *133* (17), 6728−6735.
(6) Choi, Y.; Sinev, I.; Mistry, H.; Zegkinoglou, I.; Roldan Cuenya, B. Probing the Dynamic Structure and Chemical State of Au Nanocatalysts during the Electrochemical Oxidation of 2-Propanol. *ACS Catal.* **2016**, *6* (5), 3396−3403.
(7) Arán-Ais, R. M.; Vidal-Iglesias, F. J.; Solla-Gullón, J.; Herrero, E.; Feliu, J. M. Electrochemical Characterization of Clean Shape-Controlled Pt Nanoparticles Prepared in Presence of Oleylamine/Oleic Acid. *Electroanalysis* **2015**, *27* (4), 945−956.
(8) Montiel, M. A.; Vidal-Iglesias, F. J.; Montiel, V.; Solla-Gullón, J. Electrocatalysis on Shape-Controlled Metal Nanoparticles: Progress in Surface Cleaning Methodologies. *Curr. Opin. Electrochem.* **2017**, *1* (1), 34−39.
(9) Chen, Y. X.; Miki, A.; Ye, S.; Sakai, H.; Osawa, M. Formate, an Active Intermediate for Direct Oxidation of Methanol on Pt Electrode. *J. Am. Chem. Soc.* **2003**, *125* (13), 3680−3681.
(10) Morallon, E.; Rodes, A.; Vazquez, J. L.; Perez, J. M. Voltammetric and In-Situ FTIR Spectroscopic Study of the Oxidation of Methanol on Pt (Hkl) in Alkaline Media. *J. Electroanal. Chem.* **1995**, *391* (1−2), 149−157.
(11) Rhee, C. K.; Kim, B.-J.; Ham, C.; Kim, Y.-J.; Song, K.; Kwon, K. Size Effect of Pt Nanoparticle on Catalytic Activity in Oxidation of Methanol and Formic Acid: Comparison to Pt (111), Pt (100), and Polycrystalline Pt Electrodes. *Langmuir* **2009**, *25* (12), 7140−7147.
(12) Han, S. B.; Song, Y. J.; Lee, J. M.; Kim, J. Y.; Park, K. W. Platinum Nanocube Catalysts for Methanol and Ethanol Electro-oxidation. *Electrochem. Commun.* **2008**, *10* (7), 1044−1047.
(13) Solla-Gullon, J.; Vidal-Iglesias, F. J.; Lopez-Cudero, A.; Garnier, E.; Feliu, J. M.; Aldaz, A. Shape-Dependent Electrocatalysis: Methanol and Formic Acid Electrooxidation on Preferentially Oriented Pt Nanoparticles. *Phys. Chem. Chem. Phys.* **2008**, *10* (25), 3689−3698.
(14) Susut, C.; Nguyen, T. D.; Chapman, G. B.; Tong, Y. Shape and Size Stability of Pt Nanoparticles for MeOH Electro-Oxidation. *Electrochim. Acta* **2008**, *53* (21), 6135−6142.
(15) Neurock, M.; Janik, M.; Wieckowski, A. A First Principles Comparison of the Mechanism and Site Requirements for the Electrocatalytic Oxidation of Methanol and Formic Acid over Pt. *Faraday Discuss.* **2009**, *140*, 363−378.
(16) Cuesta, A. At Least Three Contiguous Atoms Are Necessary for CO Formation during Methanol Electrooxidation on Platinum. *J. Am. Chem. Soc.* **2006**, *128* (41), 13332−13333.
(17) Housmans, T. H. M.; Koper, M. T. M. Methanol Oxidation on Stepped Pt [n (111)×(110)] Electrodes: A Chronoamperometric Study. *J. Phys. Chem. B* **2003**, *107* (33), 8557−8567.
(18) Zhang, Z.; Hui, J.; Liu, Z.-C.; Zhang, X.; Zhuang, J.; Wang, X. Glycine-Mediated Syntheses of Pt Concave Nanocubes with High-Index {hk 0} Facets and Their Enhanced Electrocatalytic Activities. *Langmuir* **2012**, *28* (42), 14845−14848.
(19) Lee, S. W.; Chen, S.; Sheng, W.; Yabuuchi, N.; Kim, Y.-T.; Mitani, T.; Vescovo, E.; Shao-Horn, Y. Roles of Surface Steps on Pt Nanoparticles in Electro-Oxidation of Carbon Monoxide and Methanol. *J. Am. Chem. Soc.* **2009**, *131* (43), 15669−15677.
(20) Li, Y.; Jiang, Y.; Chen, M.; Liao, H.; Huang, R.; Zhou, Z.; Tian, N.; Chen, S.; Sun, S. Electrochemically Shape-Controlled Synthesis of Trapezohedral Platinum Nanocrystals with High Electrocatalytic Activity. *Chem. Commun.* **2012**, *48* (76), 9531−9533.
(21) Chen, G.; Tan, Y.; Wu, B.; Fu, G.; Zheng, N. Carbon Monoxide-Controlled Synthesis of Surface-Clean Pt Nanocubes with High Electrocatalytic Activity. *Chem. Commun.* **2012**, *48* (22), 2758−2760.
(22) Chen, J.; Mao, J.; Zhao, J.; Ren, M.; Wei, M. Surfactant-Free Platinum Nanocubes with Greatly Enhanced Activity towards Methanol/Ethanol Electrooxidation. *RSC Adv.* **2014**, *4* (55), 28832−28835.
(23) Arjona, N.; Guerra-Balcázar, M.; Ortiz-Frade, L.; Osorio-Monreal, G.; Álvarez-Contreras, L.; Ledesma-García, J.; Arriaga, L. G. Electrocatalytic Activity of Well-Defined and Homogeneous Cubic-Shaped Pd Nanoparticles. *J. Mater. Chem. A* **2013**, *1* (48), 15524−15529.
(24) Qin, Y.-L.; Zhang, X.-B.; Wang, J.; Wang, L.-M. Rapid and Shape-Controlled Synthesis of "Clean" Star-like and Concave Pd Nanocrystallites and Their High Performance toward Methanol Oxidation. *J. Mater. Chem.* **2012**, *22* (30), 14861−14863.
(25) Kannan, P.; Maiyalagan, T.; Opallo, M. One-Pot Synthesis of Chain-like Palladium Nanocubes and Their Enhanced Electrocatalytic Activity for Fuel-Cell Applications. *Nano Energy* **2013**, *2* (5), 677−687.
(26) Klein, J.; Brimaud, S.; Engstfeld, A. K.; Behm, R. J. Atomic Scale Insights on the Electronic and Geometric Effects in the Electro-Oxidation of CO on PtxRu1-x/Ru (0001) Surface Alloys. *Electrochim. Acta* **2019**, *306*, 516−528.
(27) Huang, L.; Zhang, X.; Wang, Q.; Han, Y.; Fang, Y.; Dong, S. Shape-Control of Pt−Ru Nanocrystals: Tuning Surface Structure for Enhanced Electrocatalytic Methanol Oxidation. *J. Am. Chem. Soc.* **2018**, *140* (3), 1142−1147.
(28) Bai, L. Synthesis of PtRu/Ru Heterostructure for Efficient Methanol Electrooxidation: The Role of Extra Ru. *Appl. Surf. Sci.* **2018**, *433*, 279−284.
(29) Liu, H.-X.; Tian, N.; Brandon, M. P.; Zhou, Z.-Y.; Lin, J.-L.; Hardacre, C.; Lin, W.-F.; Sun, S.-G. Tetrahexahedral Pt Nanocrystal Catalysts Decorated with Ru Adatoms and Their Enhanced Activity in Methanol Electrooxidation. *ACS Catal.* **2012**, *2* (5), 708−715.
(30) Xu, D.; Liu, Z.; Yang, H.; Liu, Q.; Zhang, J.; Fang, J.; Zou, S.; Sun, K. Solution-Based Evolution and Enhanced Methanol Oxidation Activity of Monodisperse Platinum-Copper Nanocubes. *Angew. Chem., Int. Ed.* **2009**, *48* (23), 4217−4221.
(31) Zhang, N.; Bu, L.; Guo, S.; Guo, J.; Huang, X. Screw Thread-like Platinum−copper Nanowires Bounded with High-Index Facets for Efficient Electrocatalysis. *Nano Lett.* **2016**, *16* (8), 5037−5043.
(32) Li, C.; Liu, T.; He, T.; Ni, B.; Yuan, Q.; Wang, X. Composition-Driven Shape Evolution to Cu-Rich PtCu Octahedral Alloy Nanocrystals as Superior Bifunctional Catalysts for Methanol Oxidation and Oxygen Reduction Reaction. *Nanoscale* **2018**, *10* (10), 4670−4674.
(33) Chen, Q.; Cao, Z.; Du, G.; Kuang, Q.; Huang, J.; Xie, Z.; Zheng, L. Excavated Octahedral Pt-Co Alloy Nanocrystals Built with Ultrathin Nanosheets as Superior Multifunctional Electrocatalysts for Energy Conversion Applications. *Nano Energy* **2017**, *39*, 582−589.
(34) Chen, Q.; Yang, Y.; Cao, Z.; Kuang, Q.; Du, G.; Jiang, Y.; Xie, Z.; Zheng, L. Excavated Cubic Platinum−tin Alloy Nanocrystals

DOI: 10.1021/acsenergylett.9b00565
ACS Energy Lett. 2019, 4, 1484−1495

Constructed from Ultrathin Nanosheets with Enhanced Electrocatalytic Activity. *Angew. Chem.* **2016**, *128* (31), 9167−9171.
(35) Xu, X.; Zhang, X.; Sun, H.; Yang, Y.; Dai, X.; Gao, J.; Li, X.; Zhang, P.; Wang, H.; Yu, N.; et al. Synthesis of Pt−Ni Alloy Nanocrystals with High-Index Facets and Enhanced Electrocatalytic Properties. *Angew. Chem.* **2014**, *126* (46), 12730−12735.
(36) Zhan, F.; Bian, T.; Zhao, W.; Zhang, H.; Jin, M.; Yang, D. Facile Synthesis of Pd−Pt Alloy Concave Nanocubes with High-Index Facets as Electrocatalysts for Methanol Oxidation. *CrystEngComm* **2014**, *16* (12), 2411−2416.
(37) Rizo, R.; Sebastián, D.; Rodríguez, J. L.; Lázaro, M. J.; Pastor, E. Influence of the Nature of the Carbon Support on the Activity of Pt/C Catalysts for Ethanol and Carbon Monoxide Oxidation. *J. Catal.* **2017**, *348*, 22−28.
(38) Rizo, R.; Lázaro, M. J.; Pastor, E.; Koper, M. T. M. Ethanol Oxidation on Sn-Modified Pt Single-Crystal Electrodes: New Mechanistic Insights from On-Line Electrochemical Mass Spectrometry. *ChemElectroChem* **2016**, *3* (12), 2196−2201.
(39) Busó-Rogero, C.; Herrero, E.; Feliu, J. M. Ethanol Oxidation on Pt Single-Crystal Electrodes: Surface-Structure Effects in Alkaline Medium. *ChemPhysChem* **2014**, *15* (10), 2019−2028.
(40) Busó-Rogero, C.; Solla-Gullón, J.; Vidal-Iglesias, F. J.; Herrero, E.; Feliu, J. M. Oxidation of Ethanol on Platinum Nanoparticles: Surface Structure and Aggregation Effects in Alkaline Medium. *J. Solid State Electrochem.* **2016**, *20* (4), 1095−1106.
(41) Busó-Rogero, C.; Brimaud, S.; Solla-Gullon, J.; Vidal-Iglesias, F. J.; Herrero, E.; Behm, R. J.; Feliu, J. M. Ethanol Oxidation on Shape-Controlled Platinum Nanoparticles at Different PHs: A Combined in Situ IR Spectroscopy and Online Mass Spectrometry Study. *J. Electroanal. Chem.* **2016**, *763*, 116−124.
(42) Wang, H.-F.; Liu, Z.-P. Comprehensive Mechanism and Structure-Sensitivity of Ethanol Oxidation on Platinum: New Transition-State Searching Method for Resolving the Complex Reaction Network. *J. Am. Chem. Soc.* **2008**, *130* (33), 10996−11004.
(43) Busó-Rogero, C.; Grozovski, V.; Vidal-Iglesias, F. J.; Solla-Gullón, J.; Herrero, E.; Feliu, J. M. Surface Structure and Anion Effects in the Oxidation of Ethanol on Platinum Nanoparticles. *J. Mater. Chem. A* **2013**, *1* (24), 7068−7076.
(44) Tian, N.; Zhou, Z.-Y.; Sun, S.-G.; Ding, Y.; Wang, Z. L. Synthesis of Tetrahexahedral Platinum Nanocrystals with High-Index Facets and High Electro-Oxidation Activity. *Science (Washington, DC, U. S.)* **2007**, *316* (5825), 732−735.
(45) Zhou, Z.-Y.; Shang, S.-J.; Tian, N.; Wu, B.-H.; Zheng, N.-F.; Xu, B.-B.; Chen, C.; Wang, H.-H.; Xiang, D.-M.; Sun, S.-G. Shape Transformation from Pt Nanocubes to Tetrahexahedra with Size near 10 Nm. *Electrochem. Commun.* **2012**, *22*, 61−64.
(46) Lee, Y. W.; Kim, M.; Kang, S. W.; Han, S. W. Polyhedral Bimetallic Alloy Nanocrystals Exclusively Bound by {110} Facets: Au−Pd Rhombic Dodecahedra. *Angew. Chem., Int. Ed.* **2011**, *50* (15), 3466−3470.
(47) Kim, D.; Lee, Y. W.; Lee, S. B.; Han, S. W. Convex Polyhedral Au@ Pd Core−shell Nanocrystals with High-index Facets. *Angew. Chem., Int. Ed.* **2012**, *51* (1), 159−163.
(48) Zhang, J.; Hou, C.; Huang, H.; Zhang, L.; Jiang, Z.; Chen, G.; Jia, Y.; Kuang, Q.; Xie, Z.; Zheng, L. Surfactant-Concentration-Dependent Shape Evolution of Au−Pd Alloy Nanocrystals from Rhombic Dodecahedron to Trisoctahedron and Hexoctahedron. *Small* **2013**, *9* (4), 538−544.
(49) Tian, N.; Zhou, Z.-Y.; Yu, N.-F.; Wang, L.-Y.; Sun, S.-G. Direct Electrodeposition of Tetrahexahedral Pd Nanocrystals with High-Index Facets and High Catalytic Activity for Ethanol Electrooxidation. *J. Am. Chem. Soc.* **2010**, *132* (22), 7580−7581.
(50) Yu, N.; Tian, N.; Zhou, Z.; Huang, L.; Xiao, J.; Wen, Y.; Sun, S. Electrochemical Synthesis of Tetrahexahedral Rhodium Nanocrystals with Extraordinarily High Surface Energy and High Electrocatalytic Activity. *Angew. Chem., Int. Ed.* **2014**, *53* (20), 5097−5101.
(51) Cui, G.; Song, S.; Shen, P. K.; Kowal, A.; Bianchini, C. First-Principles Considerations on Catalytic Activity of Pd toward Ethanol Oxidation. *J. Phys. Chem. C* **2009**, *113* (35), 15639−15642.
(52) Yuan, Q.; Zhou, Z.; Zhuang, J.; Wang, X. Seed Displacement, Epitaxial Synthesis of Rh/Pt Bimetallic Ultrathin Nanowires for Highly Selective Oxidizing Ethanol to CO2. *Chem. Mater.* **2010**, *22* (7), 2395−2402.
(53) Rizo, R.; Arán-Ais, R. M.; Padgett, E.; Muller, D. A.; Lázaro, M. J.; Solla-Gullón, J.; Feliu, J. M.; Pastor, E.; Abruña, H. D. Pt-Richcore/Sn-Richsubsurface/Ptskin Nanocubes As Highly Active and Stable Electrocatalysts for the Ethanol Oxidation Reaction. *J. Am. Chem. Soc.* **2018**, *140* (10), 3791−3797.
(54) Zheng, Y.; Qiao, J.; Yuan, J.; Shen, J.; Wang, A.; Huang, S. Controllable Synthesis of PtPd Nanocubes on Graphene as Advanced Catalysts for Ethanol Oxidation. *Int. J. Hydrogen Energy* **2018**, *43* (10), 4902−4911.
(55) Rao, L.; Jiang, Y.-X.; Zhang, B.-W.; Cai, Y.-R.; Sun, S.-G. High Activity of Cubic PtRh Alloys Supported on Graphene towards Ethanol Electrooxidation. *Phys. Chem. Chem. Phys.* **2014**, *16* (27), 13662−13671.
(56) Antoniassi, R. M.; Silva, J. C. M.; Neto, A. O.; Spinacé, E. V. Synthesis of Pt+ SnO2/C Electrocatalysts Containing Pt Nanoparticles with Preferential (100) Orientation for Direct Ethanol Fuel Cell. *Appl. Catal., B* **2017**, *218*, 91−100.
(57) Erini, N.; Beermann, V.; Gocyla, M.; Gliech, M.; Heggen, M.; Dunin-Borkowski, R. E.; Strasser, P. The Effect of Surface Site Ensembles on the Activity and Selectivity of Ethanol Electrooxidation by Octahedral PtNiRh Nanoparticles. *Angew. Chem.* **2017**, *129* (23), 6633−6638.
(58) Liu, P.; Cheng, Z.; Ma, L.; Zhang, M.; Qiu, Y.; Chen, M.; Cheng, F. Cuprous Oxide Template Synthesis of Hollow-Cubic Cu 2 O@ Pd x Ru y Nanoparticles for Ethanol Electrooxidation in Alkaline Media. *RSC Adv.* **2016**, *6* (80), 76684−76690.
(59) Grozovski, V.; Climent, V.; Herrero, E.; Feliu, J. M. Intrinsic Activity and Poisoning Rate for HCOOH Oxidation on Platinum Stepped Surfaces. *Phys. Chem. Chem. Phys.* **2010**, *12* (31), 8822−8831.
(60) Zhang, X.; Yin, H.; Wang, J.; Chang, L.; Gao, Y.; Liu, W.; Tang, Z. Shape-Dependent Electrocatalytic Activity of Monodispersed Palladium Nanocrystals toward Formic Acid Oxidation. *Nanoscale* **2013**, *5* (18), 8392−8397.
(61) Zhang, H.-X.; Wang, H.; Re, Y.-S.; Cai, W.-B. Palladium Nanocrystals Bound by {110} or {100} Facets: From One Pot Synthesis to Electrochemistry. *Chem. Commun.* **2012**, *48* (67), 8362−8364.
(62) Jin, M.; Zhang, H.; Xie, Z.; Xia, Y. Palladium Nanocrystals Enclosed by {100} and {111} Facets in Controlled Proportions and Their Catalytic Activities for Formic Acid Oxidation. *Energy Environ. Sci.* **2012**, *5* (4), 6352−6357.
(63) Shao, M.; Odell, J.; Humbert, M.; Yu, T.; Xia, Y. Electrocatalysis on Shape-Controlled Palladium Nanocrystals: Oxygen Reduction Reaction and Formic Acid Oxidation. *J. Phys. Chem. C* **2013**, *117* (8), 4172−4180.
(64) Zheng, W.; Qu, J.; Hong, X.; Tedsree, K.; Tsang, S. C. E. Probing the Size and Shape Effects of Cubic-and Spherical-Shaped Palladium Nanoparticles in the Electrooxidation of Formic Acid. *ChemCatChem* **2015**, *7* (23), 3826−3831.
(65) Shao, Z.; Zhu, W.; Wang, H.; Yang, Q.; Yang, S.; Liu, X.; Wang, G. Controllable Synthesis of Concave Nanocubes, Right Bipyramids, and 5-Fold Twinned Nanorods of Palladium and Their Enhanced Electrocatalytic Performance. *J. Phys. Chem. C* **2013**, *117* (27), 14289−14294.
(66) Lv, T.; Wang, Y.; Choi, S.; Chi, M.; Tao, J.; Pan, L.; Huang, C. Z.; Zhu, Y.; Xia, Y. Controlled Synthesis of Nanosized Palladium Icosahedra and Their Catalytic Activity towards Formic-Acid Oxidation. *ChemSusChem* **2013**, *6* (10), 1923−1930.
(67) Tang, Y.; Edelmann, R. E.; Zou, S. Length Tunable Penta-Twinned Palladium Nanorods: Seedless Synthesis and Electrooxidation of Formic Acid. *Nanoscale* **2014**, *6* (11), 5630−5633.
(68) Choi, S.; Herron, J. A.; Scaranto, J.; Huang, H.; Wang, Y.; Xia, X.; Lv, T.; Park, J.; Peng, H.; Mavrikakis, M.; et al. A Comprehensive Study of Formic Acid Oxidation on Palladium Nanocrystals with

DOI: 10.1021/acsenergylett.9b00565
ACS Energy Lett. 2019, 4, 1484−1495

Different Types of Facets and Twin Defects. *ChemCatChem* **2015**, *7* (14), 2077−2084.
(69) Lu, B.-A.; Du, J.-H.; Sheng, T.; Tian, N.; Xiao, J.; Liu, L.; Xu, B.-B.; Zhou, Z.-Y.; Sun, S.-G. Hydrogen Adsorption-Mediated Synthesis of Concave Pt Nanocubes and Their Enhanced Electrocatalytic Activity. *Nanoscale* **2016**, *8* (22), 11559−11564.
(70) Busó-Rogero, C.; Perales-Rondón, J. V.; Farias, M. J. S.; Vidal-Iglesias, F. J.; Solla-Gullon, J.; Herrero, E.; Feliu, J. M. Formic Acid Electrooxidation on Thallium-Decorated Shape-Controlled Platinum Nanoparticles: An Improvement in Electrocatalytic Activity. *Phys. Chem. Chem. Phys.* **2014**, *16* (27), 13616−13624.
(71) López-Cudero, A.; Vidal-Iglesias, F. J.; Solla-Gullón, J.; Herrero, E.; Aldaz, A.; Feliu, J. M. Formic Acid Electrooxidation on Bi-Modified Polyoriented and Preferential (111) Pt Nanoparticles. *Phys. Chem. Chem. Phys.* **2009**, *11* (2), 416−424.
(72) Vidal-Iglesias, F. J.; López-Cudero, A.; Solla-Gullón, J.; Feliu, J. M. Towards More Active and Stable Electrocatalysts for Formic Acid Electrooxidation: Antimony-decorated Octahedral Platinum Nanoparticles. *Angew. Chem., Int. Ed.* **2013**, *52* (3), 964−967.
(73) Vidal-Iglesias, F. J.; López-Cudero, A.; Solla-Gullón, J.; Aldaz, A.; Feliu, J. M. Pd-Modified Shape-Controlled Pt Nanoparticles towards Formic Acid Electrooxidation. *Electrocatalysis* **2012**, *3* (3−4), 313−323.
(74) Jia, Y.; Jiang, Y.; Zhang, J.; Zhang, L.; Chen, Q.; Xie, Z.; Zheng, L. Unique Excavated Rhombic Dodecahedral PtCu3 Alloy Nanocrystals Constructed with Ultrathin Nanosheets of High-Energy {110} Facets. *J. Am. Chem. Soc.* **2014**, *136* (10), 3748−3751.
(75) Chen, Q.-S.; Zhou, Z.-Y.; Vidal-Iglesias, F. J.; Solla-Gullón, J.; Feliu, J. M.; Sun, S.-G. Significantly Enhancing Catalytic Activity of Tetrahexahedral Pt Nanocrystals by Bi Adatom Decoration. *J. Am. Chem. Soc.* **2011**, *133* (33), 12930−12933.
(76) Deng, Y.-J.; Tian, N.; Zhou, Z.-Y.; Huang, R.; Liu, Z.-L.; Xiao, J.; Sun, S.-G. Alloy Tetrahexahedral Pd−Pt Catalysts: Enhancing Significantly the Catalytic Activity by Synergy Effect of High-Index Facets and Electronic Structure. *Chem. Sci.* **2012**, *3* (4), 1157−1161.
(77) Zhang, Z.-C.; Hui, J.-F.; Guo, Z.-G.; Yu, Q.-Y.; Xu, B.; Zhang, X.; Liu, Z.-C.; Xu, C.-M.; Gao, J.-S.; Wang, X. Solvothermal Synthesis of Pt−Pd Alloys with Selective Shapes and Their Enhanced Electrocatalytic Activities. *Nanoscale* **2012**, *4* (8), 2633−2639.
(78) Liu, H.-X.; Tian, N.; Brandon, M. P.; Pei, J.; Huangfu, Z.-C.; Zhan, C.; Zhou, Z.-Y.; Hardacre, C.; Lin, W.-F.; Sun, S.-G. Enhancing the Activity and Tuning the Mechanism of Formic Acid Oxidation at Tetrahexahedral Pt Nanocrystals by Au Decoration. *Phys. Chem. Chem. Phys.* **2012**, *14* (47), 16415−16423.
(79) Sneed, B. T.; Brodsky, C. N.; Kuo, C.-H.; Lamontagne, L. K.; Jiang, Y.; Wang, Y.; Tao, F.; Huang, W.; Tsung, C.-K. Nanoscale-Phase-Separated Pd−Rh Boxes Synthesized via Metal Migration: An Archetype for Studying Lattice Strain and Composition Effects in Electrocatalysis. *J. Am. Chem. Soc.* **2013**, *135* (39), 14691−14700.
(80) Kuo, C.; Lamontagne, L. K.; Brodsky, C. N.; Chou, L.; Zhuang, J.; Sneed, B. T.; Sheehan, M. K.; Tsung, C. The Effect of Lattice Strain on the Catalytic Properties of Pd Nanocrystals. *ChemSusChem* **2013**, *6* (10), 1993−2000.
(81) Zhang, L.; Choi, S.; Tao, J.; Peng, H.; Xie, S.; Zhu, Y.; Xie, Z.; Xia, Y. Pd−Cu Bimetallic Tripods: A Mechanistic Understanding of the Synthesis and Their Enhanced Electrocatalytic Activity for Formic Acid Oxidation. *Adv. Funct. Mater.* **2014**, *24* (47), 7520−7529.
(82) Grosse, P.; Gao, D.; Scholten, F.; Sinev, I.; Mistry, H.; Roldan Cuenya, B. Dynamic Changes in the Structure, Chemical State and Catalytic Selectivity of Cu Nanocubes during CO2 Electroreduction: Size and Support Effects. *Angew. Chem., Int. Ed.* **2018**, *57* (21), 6192−6197.

DOI: 10.1021/acsenergylett.9b00565
ACS Energy Lett. 2019, 4, 1484−1495